Sequential Sampling Algorithm for Simultaneous Near-Field Scanning of Amplitude and Phase

Tim Claeys, Davy Pissoort
Laboratory FMEC
Reliability in Mechatronics and ICT Research Group
KU Leuven, campus Kulab
Zeedijk 101, B-8400 Oostende (Belgium)
Corresponding author: tim.claeys@kuleuven.be

Dirk Deschrijver, Ivo Couckuyt, Tom Dhaene
SUMO Research Lab
Dept. of information Technology
Ghent University - iMinds
Gaston Crommenlaan 8, B-9050 Ghent (Belgium)

***Abstract*—This paper describes an automated sequential sampling algorithm for EMI near-field scanning of electronic systems which allows to measure both magnitude and phase of the electromagnetic near-fields simultaneously. The main goal of the sequential sampling algorithm is to drastically reduce the total measurement time to obtain a complete model of the electronic system's near-field distribution. Measuring both magnitude and phase is important for predicting the far-field emission from the near-field or for building equivalent radiation models of the device under test. Previous work described such a sequential sampling algorithm for amplitude-only measurements. The extension towards both amplitude and phase poses two challenges. First, the underlying sampling and modelling techniques have to be adapted such that they can handle building up two separate models at the same time using a common set of optimal sampling points and without significant increase of the measurement time. Second, a good choice has to be made with respect to which components will be sampled and modelled. It is shown that the most advantageous choice is to sample and model the real and imaginary components of the near-fields instead of the amplitude and phase directly.**

***Index Terms*—Electromagnetic compability; near field scanning; surrogate modeling; kriging**

I. Introduction

Every day a new electronic system is developed which functionality and speed is increased and which is squeezed into an even smaller area compared to previous electronic systems. A down side of this phenomenon is the increasing chance of Electro-Magnetic Interference (EMI) problems. For the most-effective design, EMI should be taken into account in every step of the design process. When a first prototype is available, it can be tested for its radiated emissions in a (semi-) anechoic chamber, a reverberation chamber or at an open area test site. Unfortunately, these test environments are very expensive and are seldom available at the company itself. Hence, EMI testing is costly and very often postponed until the very end of the design process. Moreover, these types of tests measure the radiated far-field of the device and do not directly allow to check where the radiation is originated from.

To solve this problem, a low-cost pre-certification test method that provides in-depth insight on the real root cause of excessive emissions would be very useful. Near-field (NF) scanning of the electro-magnetic fields close by the device or its components serves this goal [1]. Near-field scanning is cheap when compared to the classical methods mentioned above, and can be used in every step of the design cycle. The main disadvantage of NF scanning is the time needed for scanning the complete device under test (DUT) with sufficient resolution to capture all relevant radiation phenomena. The most common way of measuring the NF is on a cartesian grid with a small distance between the measuring points.

A first proposal to reduce the total measurement time was based on the use of a neural network to model and interpolate the near-field data [2]. In [2], The near-field data is still sampled on a cartesian grid with a pre-chosen resolution, albeit a larger one than when no modelling and interpolation is used. However, if this resolution is chosen too large, there will be a certain loss of information; if it is chosen too small, there will be a unnecessary increase of the measurement time.

A second proposal was introduced in [3] and [4]. Besides advanced modelling and interpolation, these papers introduced a sequential sampling algorithm using a balanced tradeoff between 'exploration' (Voronoi Tesselations) and 'exploitation' (Local Linear Approximations). Instead of simply sampling on a cartesian grid, the sequential sampling algorithm automatically detects the most optimal sampling locations. The modelling and interpolation is based on Kriging. It was proven that accurate results can be achieved with 8 to 10 times less sampling points compared to a Cartesian grid, thereby also reducing the measurement time drastically. In [5] this sequential sampling algorithm was further optimized by using a batch of N samples, instead of 1 sample. A second optimization was made by minimizing the traveling distance of the probe when passing through N samples in each step.

All methods above were only applied to amplitude-only measurements. In this paper, the sequential sampling algorithm with Kriging modelling is extended towards simultaneous measurement of both magnitude and phase (i.e., 2 outputs instead of 1 output). The main challenges are (i) how to choose the optimal and minimal set of sampling points to build up separate models for two components at the same time using a common set of samples and (ii) which are the best components

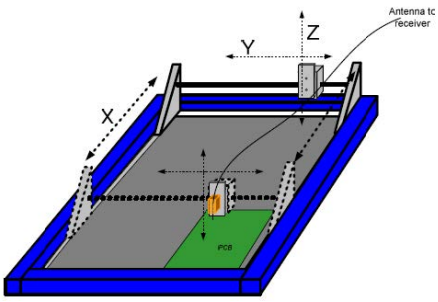

Fig. 1. Near-field scanning system

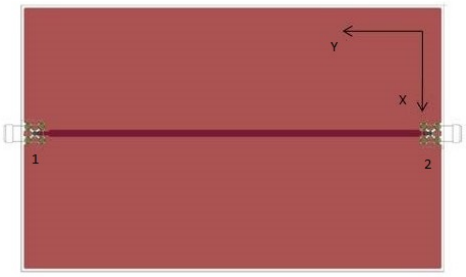

Fig. 2. Straight microstrip

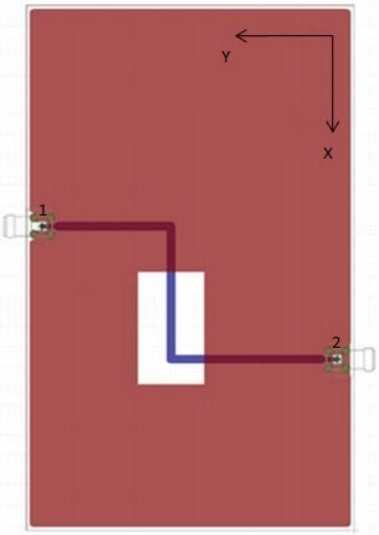

Fig. 3. Bended microstrip

to model and interpolate. With respect to the latter, two choices exist: either amplitude and phase or real and imaginary. In this paper, it will be shown that the most advantageous choice is to sample and model the real and imaginary components, as these tend to show a smoother behavior than the phase. Which is advantageous for the underlying Kriging modelling.

This paper is organized as follows. Section II gives some information about the near-field scanner, probe(s) and the used printed circuit boards (PCBs). Section III will give a brief introduction in the sequential sampling algorithm and its extension towards building up two models at the same time. Section IV shows how the measurements are done in more detail while section V will summarize all the results. Finally in Section VI concluding remarks are drawn.

II. Measurement set-up

A. Near-field scanning system and probe

Fig. 1 shows the NF scanning system available at the ReMI research group of KU Leuven Kulab, campus Ostend. The NF scanning system is built from a CNC milling machine. Its miller and suspension were removed and replaced by a holder for a near-field probe. This gives the possibility to move the probe in 3 spatial dimensions above the DUT.

The moving probe used for the measurements is a magnetic near-field probe produced by Langer EMV-Technik (RF-R 3-1) specified for the frequency range of 30 MHz up to 3 GHz. For measuring both amplitude and phase, this probe is connected to either a vector network analyzer or an oscilloscope [18]. The second (fixed) probe is a 3 cm loop magnetic near-field probe (7405-902B) from ETS-Lindgren's, with a frequency range of 100 KHz up to 1.5 GHz. Although only results for the x-component of the magnetic field at 1 GHz will be shown in this paper, similar conclusions can be drawn for the other components of the magnetic or electric field. In all cases shown below, the measurement height was 4 mm above the DUT.

B. PCBs under test

In this paper, 2 PCBs are considered. The first PCB (Fig. 2) is a simple 50Ω microstrip on a 16 cm by 10 cm two-sided FR4 substrate of 1.5 mm thickness. The second PCB (Fig. 3) comprises a 50Ω microstrip with two 90 degree bends. In order to have larger radiation, the microstrip is routed above a rectangular slot in the ground-plane. All microstrips are excited at one end and terminated with 50Ω at the other end.

III. Sequential sampling algorithm for two simultaneous models

The sequential sampling algorithm proposed in [3] and [4] starts by computing a small number of initial scan points according to an optimized Latin hypercube design [9]. In successive steps, additional sampling points are selected one by one in a sequential way until the overall variation of the NF pattern is characterized. In order to sample the NF pattern as efficiently as possible, the robust sampling strategy from [10]-[12] is applied to determine optimal coordinates of the sampling points in a sequential way [13]-[15]. The sampling algorithm makes a balanced trade-off between exploration and exploitation criteria:

- Exploration is the act of exploring the design space in order to detect key regions that have not yet been identified before. It does not involve the actual pattern of the near-fields, but only the coordinates of the sampling

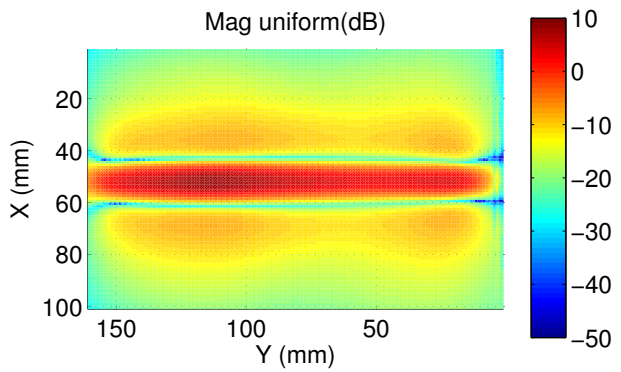

Fig. 4. Straight PCB: Uniform sampling, Magnitude

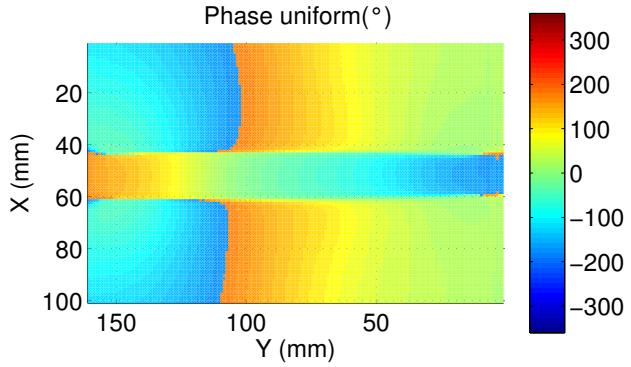

Fig. 5. Straight PCB: Uniform sampling, Phase

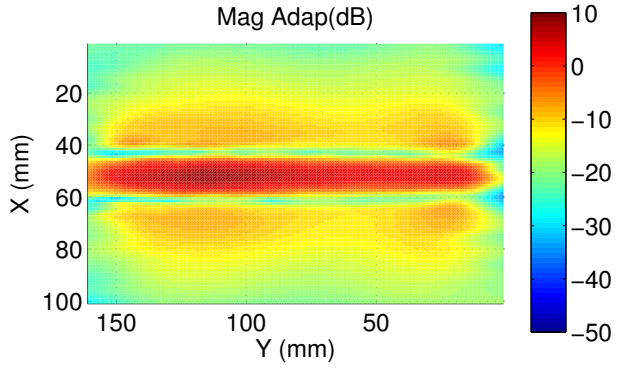

Fig. 6. Straight PCB: Adaptive-M sampling, Magnitude

points and their coverage of the design space. It ensures that all the scan points are spread as evenly as possible.
- Exploitation ensures that additional scans are performed in regions of the design space where the amplitude of the near-field component that is being measured is changing more rapidly. These regions often require a finer sampling density than regions with little variation.

Based on a Voronoi tesselation, the design space is divided into a set of disjoint cells. For each cell C_k that corresponds to a scan point having coordinate vector $\vec{x}_k$, two different metrics are computed. The first metric $V(\vec{x}_k)$ assesses the density of samples around the given point $\vec{x}_k$, whereas the second metric $W(\vec{x}_k)$ quantifies the portion of the dynamic variation in the NF pattern that is located near the cell. Both metrics are summed into a global metric $G(\vec{x}_k)$ that is used for ranking the cells, and additional points are chosen within the highest ranked cell. All details are discussed in Section III of [3].

In order to deal with 2 outputs, the algorithm needs a modification. Since each output should be measured at the same coordinates, the subdivision into Voronoi cells and their score $V(x_k)$ will be the same. However, note that the score $W(x_k)$ will be different, because the dynamic variation between magnitude and phase, or real and imaginary part of the NF pattern is different. In order to compute $G(x_k)$, one simply uses the worst-case (i.e. largest) value of $W(x_k)$. Samples are again chosen inside the highest ranked cell.

Once a set of data samples is obtained from the sequential sampling algorithm, an analytic approximation model can be computed by Kriging. Kriging, also known as Gaussian Process regression, is a geostatical modeling technique that originates from geology and mining [16]. In theory, one could build a Kriging approximation model after every sample is measured, although this is not the most efficient way of measuring the near-field pattern [5]. Instead, a total number of 350 samples are measured in batches of 15 samples. All measurements in this paper were made using these settings.

IV. Measurement workflow

In this section a workflow is introduced so that a reasonable comparison can be made between different measurements. First the measurement method with the Vector Network Analyzer (VNA) is discussed. This method presented in [18], can measure most practical PCB's which are self-powered. The VNA has the ability to measure the ratio between two complex signals directly. Using this, one can measure the ratio (magnitude and phase) between two measuring probes. One of these probes is at a fixed position, whilst the other one acts as the moving probe. When measuring the PCBs, the adaptive sampling algorithm was then used for 3 independent runs:

- In the first run, measurements were performed by adaptively sampling the magnitude only (Adaptive-M) [5].
- In the second run, both magnitude and phase are simultaneously sampled in an adaptive way (Adaptive-MP).
- In the third run, both real and imaginary part are simultaneously sampled in an adaptive way (Adaptive-RI).

In order to assess the model accuracy, the mean value of the difference between the model predictions and a very dense set of uniform measurements is computed as in equation (1). These uniform measurements were performed over an equispaced grid of 1 mm (16261 sample points), and serve as a reference or validation set to quantify the goodness of the models. It is not the intention for defining a correct error value but rather to assign a value wich can indicate the difference

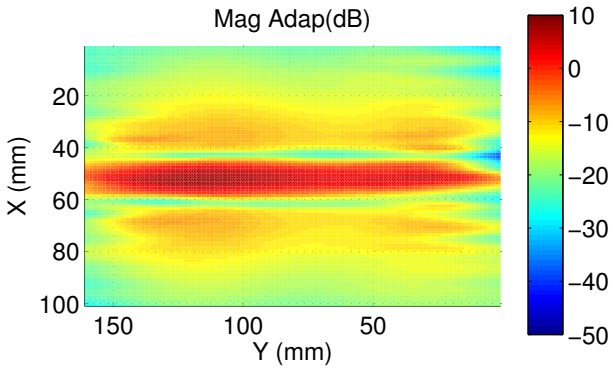

Fig. 7. Straight PCB: Adaptive-MP sampling, Magnitude

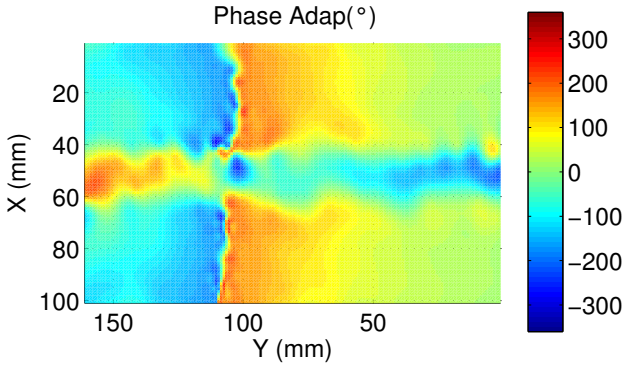

Fig. 8. Straight PCB: Adaptive-MP sampling, Phase

	Mag Error	Phase Error (°)
Adaptive-M	0.58	/
Adaptive-MP	0.96	16.5156
Adaptive-RI	0.23	1.94

TABLE I
ERROR STRAIGHT MICROSTRIP

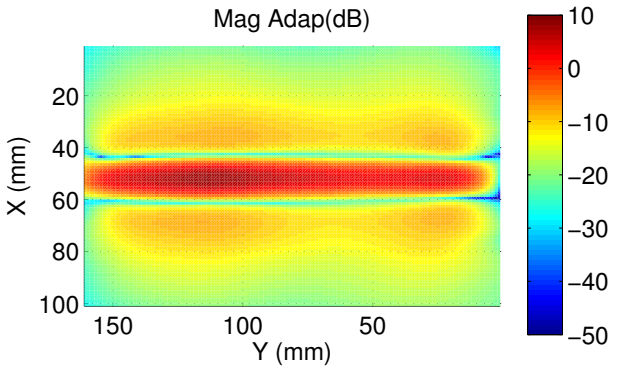

Fig. 9. Straight PCB: Adaptive-RI sampling, Magnitude

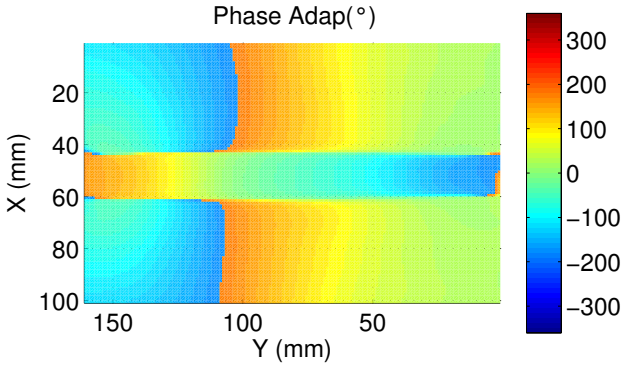

Fig. 10. Straight PCB: Adaptive-RI sampling, Phase

	Mag Error	Phase Error (°)
Adaptive-M	0.99	/
Adaptive-MP	1.11	21.46
Adaptive-RI	0.66	6.35

TABLE II
ERROR BENDED MICROSTRIP

between the uniform and adaptive sampling, so that a low error value will result in a better model then a large value.

$$\frac{1}{n}\sum_{i=1}^{n} \mid Uni - Adap \mid \qquad (1)$$

V. MEASUREMENT RESULTS

As explained in the previous section, there will be 3 runs for each PCB. First the results of the uniform measurement are shown in Figures 4 & 5 for the straight PCB, whereas those for the bended PCB are shown in 11 & 12. Figures 7 & 8 and Figures 14 & 15 show the results for the Adaptive-MP sampling for the straight and bended PCB respectively. Analogously, the results for the Adaptive-RI sampling are shown in Figures 9 & 10 and Figures 16 & 17.

Tables I and II show the corresponding error between the uniform and adaptive measurement. As can be seen from the error values and the intensity plots, it can be concluded that the best way to characterize the field is by measuring and modeling the real and imaginary parts of the data, instead of the magnitude and phase. Is it obvious that magnitude and phase can easily be reconstructed from these values. The reason for this phenomenon is found in the exploitation part of the adaptive algorithm. It focuses on regions where values change a lot and samples much finer at these points. When measuring the phase, one can see that the algorithm zooms in on phase jumps of 360 degrees, which is undesired. Such problems can easily be avoided by measuring real and imaginary parts of the complex values instead, leading to more accurate models.

An important aspect is the time needed for this adaptive sampling algorithm. A uniform measurement of the test PCB's takes up to 4 hours. An adaptive measurement with one kriging model (only magnitude) takes up to 15 minutes while two Kriging models (Magnitude/phase or Real/Imaginary) takes up to 20 minutes.

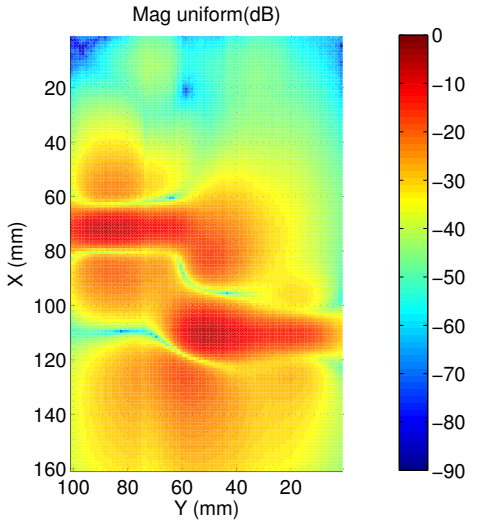

Fig. 11. Bended PCB: Uniform sampling, Magnitude

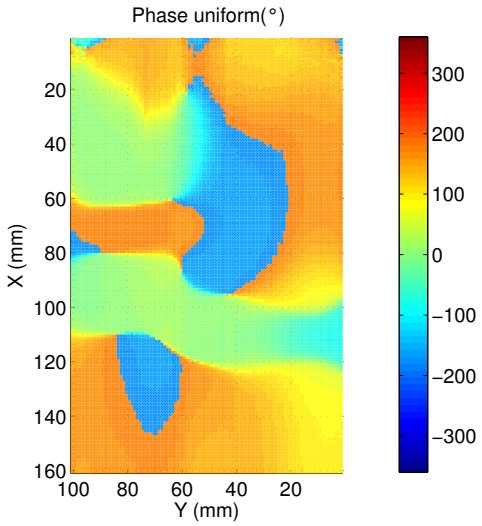

Fig. 12. Bended PCB: Uniform sampling, Phase

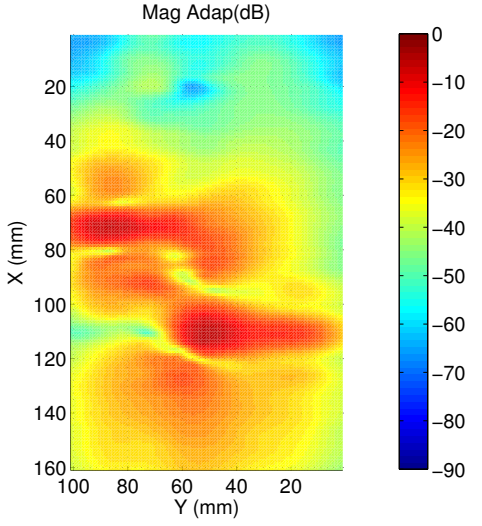

Fig. 13. Bended PCB: Adaptive-M sampling, Magnitude

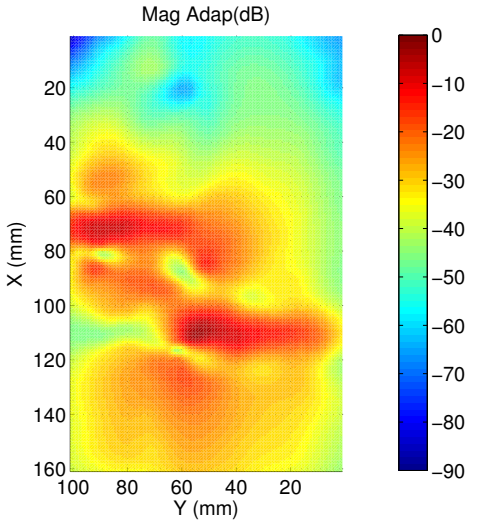

Fig. 14. Bended PCB: Adaptive-MP sampling, Magnitude

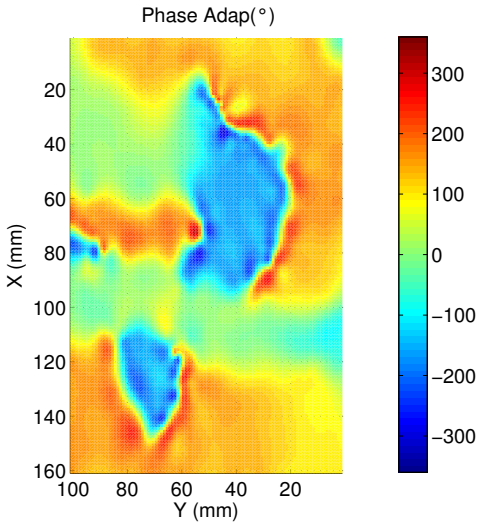

Fig. 15. Bended PCB: Adaptive-MP sampling, Phase

VI. Conclusion

A sequential sampling algorithm for the fast and accurate measurement of both magnitude and phase of the electromagnetic near-field above a DUT was proposed. The sequential sampling algorithm automatically determines a minimal set of optimal sampling points and models the real and imaginary part of the near-field. It is shown that this approach leads to more accurate results than sampling and modelling the magnitude and phase. The algorithm is effective and generalizes the methodology of measuring the magnitude only [3].

Acknowledgment

This research was supported by the IWT (Flanders, Belgium) under the TETRA-NEATH project. This work was also supported by the Research Foundation Flanders (FWO-Vlaanderen) and the Interuniversity Attraction Poles Pro-

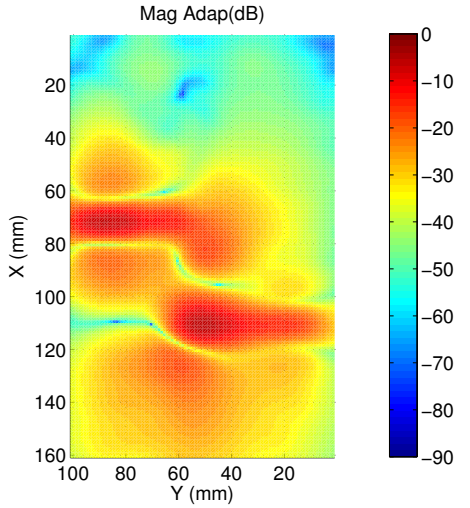

Fig. 16. Bended PCB: Adaptive-RI sampling, Magnitude

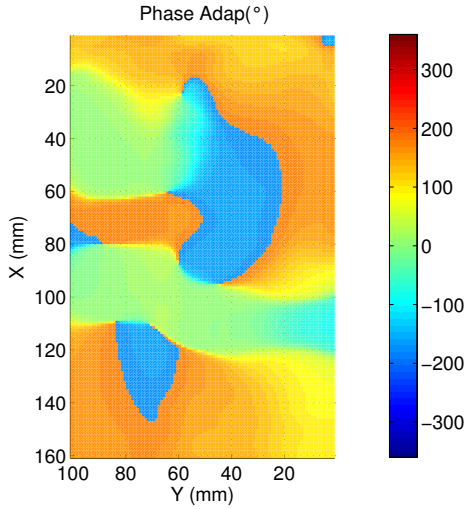

Fig. 17. Bended PCB: Adaptive-RI sampling, Phase

gramme BESTCOM initiated by the Belgian Science Policy Office. Dirk Deschrijver and Ivo Couckuyt are post-doctoral research fellows of FWO-vlaanderen.

REFERENCES

[1] D. Baudry, C. Archambal, A. Louis, B. Mazari and P. Eudeline, "Applications of the near-field techniques in EMC investigations", IEEE Transactions on EMC, vol. 49, no. 3, pp. 485-493.

[2] R. Brahimi, A. Kornaga, M. Bensetti, D. Baudry, Z. Riah, A. Louis and B. Mazari, "Postprocessing of near-field measurement based on neural networks", IEEE Transactions on Instrumentation and measurement, vol. 60, no. 2, pp. 539-546, Feb 2011.

[3] D. Deschrijver, D. Pissoort and T. Dhaene, "Automated near-field scanning algorithm for the EMC analysis of electronic devices", IEEE Transactions on EMC, vol. 54, no. 3, pp. 502-510, June 2010.

[4] B. Van der Streeck, F. Vanhee, B. Boesman, D. Pissoort, D. Deschrijver, I. Couckuyt and T. Dhaene, "Practical Implementation of a sequential sampling algorithm for EMI near-field scanning", International Symposium on Electromagnetic Compatibility (EMC Europe), Rome (Italy), pp. 1-5, September 2012.

[5] T. Dorné, F. Vanhee, T. Grenson, D. Pissoort, D. Deschrijver, I. Couckuyt and T. Dhaene, "Optimized sequential sampling algorithm for EMI near-field scanning", International Symposium on Electromagnetic Compatibility (EMC Europe 2013), Brugge (Belgium), pp. 385-388, September 2013.

[6] P.A. Barrire,J.J. Laurin and Y. Goussard, "Mapping of equivalent Currents on High-Speed Digital Printed Circuit Boards Based on Near-Field Measurements", IEEE Transactions on Electromagnetic Compability,vol.51, no.3, pp. 649-658, Aug 2009.

[7] Y. Alvarez, F. Las-Heras and M.R. Pino, "The Source Reconstruction Method for Amplitude-Only Field Measurements", IEEE transactions on Antennas and Propagation, vol. 58, no. 8, pp.2776-2781, Aug 2010.

[8] Y. Alvarez, M. Rodrguez, F. Las-Heras and M.H. Fernando, "On the Use of Source Reconstruction Method for Estimating Radiated EMI in Electronic Circuits", IEEE Transactions on Instrumentation and Measurement, vol. 59, no. 8 , pp. 3174-3183, Dec 2010.

[9] A. Forrester, A. Sobester and A. Keane,"Engineering Design via Surrogate Modelling: A Practical Guide", Wiley,2008.

[10] K. Crombecq, D. Gorissen, L. De Tommasi and T. Dhaene, "A Novel Sequential Design Strategy for Global Surrogate Modeling", Proceedings 41th Conference on Winter Simulation, pp. 731-742,2009.

[11] K. Crombecq, D. Gorissen, D. Deschrijver and T. Dhaene, "A Hybrid Sequential Design Strategy for Global Surrogate Modeling of Computer Experiments", SIAM journal on Scientific Computing (SISC), Vol. 33, No. 4, pp. 1948-1974, July-August 2011.

[12] D. Deschrijver, K. Crombecq, H.M. Nguyen and T. Dhaene, "Adaptive Sampling Algorithm for Macromodeling of Parameterized S-Parameter Responses", IEEE Transactions on Microwave Theory and Techniques, vol. 59, no. 1,pp. 39-45, Jan 2011.

[13] P. Singh, D. Deschrijver, D. Pissoort, T. Dhaene, "Accurate Hotspot Localization by Sampling the Near-Field Pattern of Electronic Devices", IEEE Transactions on Electromagnetic Compatibility, vol. 55, no. 6, pp. 1365-1368, December 2013.

[14] S. Aerts, D. Deschrijver, W. Joseph, L. Verloock, F. Goeminne, L. Martens, T. Dhaene, "Exposure Assessment of Mobile Phone Base Station Radiation in an Outdoor Environment using Sequential Surrogate Modeling", Bioelectromagnetics, vol. 34, no. 3, pp. 300-311, May 2013.

[15] P. Singh, D. Deschrijver, D. Pissoort, T. Dhaene, "Adaptive Classification Algorithm for EMC Compliance Testing of Electronic Devices", IEE Electronics Letters, vol. 49, no. 24, pp. 1526-1528, 2013.

[16] M. A. Oliver and R. Webster, "Kriging: a method of interpolation for geographical information system", International Journal of Geographical Information Systems, vol. 4, no. 3, pp. 313-332, 1990.

[17] D. Gorissen, K. Crombecq, I. Couckuyt, T. Dhaene and P. Demeester,"A surrogate Modeling and Adaptive Sampling Toolbox for computer Based Design", Journal of Machine Learning, vol. 11, pp. 2051-2055, Jul 2010.

[18] X. Tong, (2010), Simplified Equivalent Modelling of Electromagnetic Emissions from Printed Circuit Boards, Ph.D thesis, University of Nottingham, U.K.

[19] Surrogate Modeling Toolbox v. 7.0, http://sumo.intec.ugent.be, Ghent University - iminds, Ghent (Belgium), Mar 2011.